

## Mesh Collapse in Two-Dimensional Elastic Networks under Compression

Wolfgang Wintz <sup>(1)</sup>, Ralf Everaers <sup>(2)</sup> and Udo Seifert <sup>(1,\*)</sup>

<sup>(1)</sup> Max-Planck-Institut für Kolloid- und Grenzflächenforschung, Kantstrasse 55, 14513 Teltow-Seehof, Germany

<sup>(2)</sup> Institut Charles Sadron, 6, rue Boussingault, 67083 Strasbourg, France

(Received 19 November 1996, revised 18 February 1997, accepted 15 May 1997)

PACS.46.30.Cn – Static elasticity

PACS.62.20.Dc – Elasticity, elastic constants

PACS.87.22.Bt – Membrane and subcellular physics and structure

**Abstract.** — We consider two-dimensional triangular networks of beads connected by Hookean tethers under isotropic compression. We determine both the compression and the shear modulus as a function of temperature and compression within simple approximations and by a Monte Carlo simulation. At low temperature, this network undergoes a collapse transition with increasing compression. In the two phase region, collapsed and non-collapsed triangles coexist. While the compression modulus vanishes in the two phase region, the shear modulus shows only a small anomaly at the transition. With increasing temperature, this transition disappears in our simulation. Anharmonic shear fluctuations invalidate a harmonic analysis in large regions of the phase space. In application to the red blood cell membrane, we obtain good agreement with more microscopic models for the shear modulus. Our results also indicate that strong compression will lead to non-trivial elastic behavior of the cell membrane.

### 1. Introduction

Models, consisting of systems of identical connected springs, are commonly used to explain the mechanical properties of elastic materials. One-dimensional chains embedded in higher dimensional space have been intensively examined in the fields of polymer physics [1]. Two-dimensional spring networks have been investigated as models of polymerized membranes [2]. The fundamental material parameters of such a network (as long as it is isotropic) are the compressibility and the shear modulus. If the network is not confined to two dimensions but rather allowed to explore the third dimension, a third parameter, namely the bending rigidity, comes into play. Several studies have been devoted to strictly two-dimensional triangular networks for which the externally applied tension is a crucial parameter [3, 4]. The elastic behavior of such *stretched* networks can be understood using simple mean-field arguments. As an example for the unusual effects one encounters in two-dimensional networks, we mention a negative Poisson ratio which has been predicted by mean-field calculations and confirmed by the results of a Monte Carlo simulation [4].

---

(\*) Author for correspondence (e-mail: useifert@mpikg-teltow.mpg.de)

The purpose of this paper is to investigate two-dimensional elastic networks under *lateral compression*. A network can be compressed, if it shows both a non-vanishing equilibrium area in its relaxed state and elastic response to an external constraint imposing smaller area. Instead of buckling into the third dimension lateral compression of a network patch occurs, if the bending modulus of the system is sufficiently large compared to the product of lateral pressure and the square of the maximal diameter of the patch. The skeleton of the red blood cell (RBC) membrane is a paradigmatic but somewhat subtle realization of a two-dimensional network [5], which fulfills these two conditions for the occurrence of lateral network compression. The RBC membrane consists of a globally almost incompressible fluid lipid bilayer. Attached to this bilayer *via* integral proteins there is a closed two-dimensional, almost perfectly hexagonal network of spectrin tetramers. The connection of bilayer and net is close enough to consider the net as a constituent part of the cell membrane. In experiments, in which the skeleton is extracted from the membrane, the network shows non vanishing equilibrium area for observation times up to hours [6]. The bilayer provides the system with a sufficiently large bending resistance to allow lateral compression of network patches, which are large compared to the area of molecular meshes.

The presence of the incompressible fluid bilayer has important consequences for the tension field within the network. In particular, the network needs not to be relaxed in the equilibrium state of the membrane since the number of lipid molecules within the bilayer determines the total membrane area due to the high area expansion modulus of the bilayer. Retracting or adding lipid molecules from or to the bilayer of the RBC exerts isotropic compression or stretching on the network [7]. Furthermore, the incompressibility of the bilayer implies that any cell deformation causes, in general, local stretching, compression and shearing of the membrane skeleton.

In various experiments RBCs have been deformed by external forces in order to extract the elastic properties of the membrane. The most prominent method to exert cell deformations in a controlled manner is the use of micropipettes [8]. In these experiments parts of the membrane are aspirated into the pipette by negative pressure. The pressure-extension relation is measured together with density profiles of different components of the cell membrane [9]. The deformations applied in these experiments are quasi stationary and strong. In a second class of experiments, time sequences of the thermal fluctuations of the cell shape are recorded and analyzed [10,11]. The crucial part in the analysis of all these experiments is the decomposition of the elastic response of the membrane into contributions from the bilayer and the skeleton. For this decomposition, models that incorporate both components have to be used. The quite intricate behavior our model shows under certain conditions indicates that simple minded approaches concerning the elastic properties of the membrane skeleton may lead to an incorrect analysis of the experimental results.

The paper is organized as follows. In Section 2, we define the model and analyze stability of a single mesh at zero temperature and for finite temperature within a simple mean-field approximation. In Section 3, we present the results of a Monte Carlo simulation. In Section 4, we apply our results to models of the RBC membrane. A brief conclusion follows in Section 5.

## 2. The Model

2.1. BOND POTENTIAL. — We model the network by a two-dimensional hexagonal lattice of springs confined to a plane [4]. Thus, buckling is excluded. We also ignore defects and inhomogeneities. Each spring with length  $l_i$  is subject to a potential  $V(l_i)$ . If the springs, which model the spectrin strands, consisted of ideal Gaussian chains, the equilibrium length would be zero and the area would vanish. A non-vanishing equilibrium area can be achieved

physically by three mechanisms:

- 1) a non-vanishing equilibrium length  $l_0$  of the springs, which can be motivated from a self avoiding random walk or a worm-like chain model for the single-chain elasticity;
- 2) an isotropic internal pressure  $p_{\text{in}}$  due to the inter-chain volume interactions;
- 3) the topological constraint of having *no* entanglement between network strands, if we assume that network connectivity and surface anchoring are preserved under compression. This condition bears similarities to a three-dimensional melt of non-concatenated ring polymers [12]. The effect is incorporated into our model in a crude way by a hard wall potential which prevents the movement of vertices across bonds.

The compression of the network by external forces is achieved either by the application of external isotropic lateral pressure  $p_{\text{ex}}$  (pressure ensemble) or by periodic boundary conditions (area ensemble).

We will now analyze the statistical mechanics of such a network assuming that  $V(l)$  is independent of temperature and compression. While such a condition may not be met in a given physical system, it is a well defined model. The zero temperature equilibrium conformation of each unit cell of the network, which consists of one vertex, two triangles and three bonds of lengths  $l_i$  ( $i = 1, \dots, 3$ ), can be calculated by minimizing its energy

$$f(l_1, l_2, l_3) = \sum_{i=1}^3 V(l_i) + 2pA(l_1, l_2, l_3), \quad (1)$$

where  $p$  is the sum of internal and external pressure and  $A(l_1, l_2, l_3) \geq 0$  is the area of the triangle.

Variation of (1) with respect to the three bond-lengths gives a set of three equations that determines the stationary conformations. For an equilateral triangle, *i.e.*,  $l_1 = l_2 = l_3 = l$ , these stationarity equations reduce to  $\partial f / \partial l = 0$ . This equation determines the equilibrium length  $l_e$  by

$$\frac{\partial V}{\partial l}(l_e) + \frac{p}{\sqrt{3}} l_e = 0. \quad (2)$$

2.2. HOOKE'S LAW NETWORKS. — For a stability analysis of the equilateral conformation, we specify  $V$  to be a Hooke's law potential,

$$V(l) = \frac{k}{2}(l - l_0)^2, \quad (3)$$

where  $k$  is the spring constant and  $l_0$  the spring length. This choice for  $V(l)$  may be interpreted as the first term of a series expansion of an arbitrary potential with a single spring equilibrium length of  $l_0$ . In the following we measure  $l$  in units of  $l_0$ . Pressure will be measured in units of  $k$  and energy in units of  $kl_0^2$ .

The stationarity equations show that all stationary conformations are isosceles triangles. They can be parameterized by the length,  $l$ , of the two equal sides and  $\alpha$ , which is half the angle between them. In this parameterization, the free energy of a single unit cell becomes

$$f = 2V(l) + V(2l \sin \alpha) + 2pl^2 \sin \alpha \cos \alpha. \quad (4)$$

For negative  $p$ , the equilateral mesh ( $\alpha = \pi/6$ ) is the only and therefore stable stationary conformation. When  $p$  approaches  $-\sqrt{3}$ ,  $l_e$  grows continuously to infinity [4]. This means that

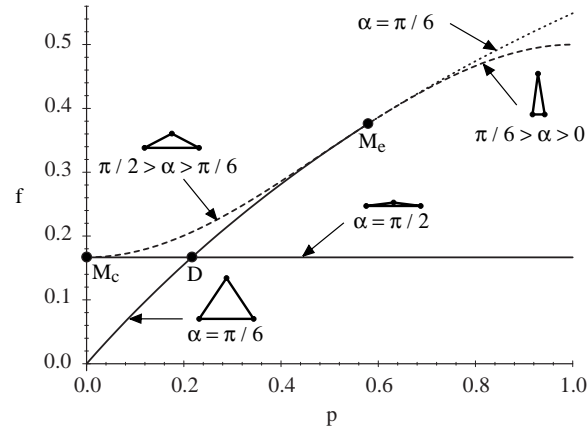


Fig. 1. — Energy  $f$  of a single mesh as a function of pressure  $p$ . Solid lines represent locally stable conformations: The equilateral ( $\alpha = \pi/6$ ) and the collapsed ( $\alpha = \pi/2$ ). At  $M_e$  ( $p = 1/\sqrt{3}$ ) the equilateral conformation becomes unstable. Both branches cross at  $D$  ( $p = \sqrt{3}/8$ ). The energy barrier between the two locally stable conformations consists of unstable, non collapsed isosceles triangles ( $\pi/2 > \alpha > \pi/6$ ). This branch continues beyond  $M_e$  ( $\alpha = \pi/6$ ) and ends at  $p = 1$  in an unstable collapsed conformation ( $\alpha = 0$ ,  $f = 1/2$ ).

the network can be infinitely expanded by the application of a finite tension. For positive  $p$ , additional stationary conformations arise. A locally stable one is a collapsed mesh with  $l = 2/3$  and  $\alpha = \pi/2$  and a free energy of  $f = 1/6$ . This state is a boundary minimum stabilized by the constraint of forbidden bond crossing.

Figure 1 shows the energy diagram for a single mesh. For  $p > 1/\sqrt{3} \simeq 0.6$  the equilateral conformation becomes unstable with respect to a shear deformation, which breaks the symmetry of the equilateral triangle. This scenario is typical for a discontinuous transition of the equilibrium conformation. It implies a first order phase transition of the network between an equilateral and a collapsed phase. The height of the energy barrier between the equilateral and the collapsed conformation is approximately 0.02.

2.3. ELASTIC RESPONSE ON STATIC DEFORMATIONS. — The values of the elastic constants for the equilateral phase of the network can be extracted from an analysis of static deformations of the equilibrium conformation [4]. The area per unit cell  $a(p)$  (measured in units of  $\sqrt{3} l_0^2/2$ ), the area compression modulus  $K_p$  and the shear modulus  $\mu_p$  (both in units of  $k$ ) depend on the pressure as follows:

$$a = (1 + p/\sqrt{3})^{-2}, \quad (5)$$

$$K_p = \frac{\sqrt{3}}{2}(1 + p/\sqrt{3}), \quad (6)$$

$$\mu_p = \frac{3}{4}(1/\sqrt{3} - p). \quad (7)$$

As mentioned above, the area  $a$  diverges at  $p = -\sqrt{3}$ . At this value,  $K_p$  vanishes. The shear modulus  $\mu_p$  vanishes at  $p = 1/\sqrt{3}$ , indicating an instability of the equilateral conformation with respect to shear deformations at  $M_e$ . The elastic constants  $K_p$  and  $\mu_p$  are meaningful quantities only for the equilateral phase. Beyond the collapse transition, where for zero temperature  $a = 0$ , they are no longer defined.

2.4. CONSTANT AREA ENSEMBLE. — Of course, a complete net collapse is impossible for the membrane skeleton because it is connected to the closed bilayer with constant surface area. Thus we have to consider a constant area ensemble rather than a constant pressure ensemble. In the constant area ensemble, coexistence of the equilateral and the collapsed phase becomes possible.

For a simple lever rule calculation, which neglects the coupling between the phases at their boundaries, we assume a binary mixture of collapsed and equilateral meshes and minimize the free energy. Varying both the ratio of collapsed and non collapsed meshes and the bond length of the equilateral triangles for a given total number of unit cells  $N$  and total area  $A$  shows that the transition will occur at constant pressure  $p = \sqrt{3}/8 \simeq 0.2$ , which corresponds to the transition D in Figure 1. The area per triangle  $a = A/N$  at the transition is 21% less than the area at  $p = 0$ . The bond length in the equilateral phase is found to be  $l_e = 8/9$ . Thus the bond length in the equilateral phase fits neither the length of the short sides of the collapsed meshes ( $2/3$ ) nor of the long sides ( $4/3$ ).

The elastic constants

$$K_A = \frac{\sqrt{3}}{2} \frac{1}{\sqrt{a}} \quad (8)$$

and

$$\mu_A = \sqrt{3} \left(1 - \frac{3}{4} \frac{1}{\sqrt{a}}\right) \quad (9)$$

follow if equation (5) is used to eliminate  $p$  from equations (6, 7). Again these equations are only valid in the equilateral regime. But in contrast to the case above,  $K_A$  and  $\mu_A$  are meaningful quantities also for the two phase regime, which does not exist in the constant pressure ensemble.

Neglecting phase boundary effects, both  $K_A$  and  $\mu_A$  vanish in the limit of zero temperature, when the system enters the two phase regime. Using the definition of  $K_A$  in the form

$$K_A = -a \frac{\partial p}{\partial a}, \quad (10)$$

this result follows from the lever rule calculation, which shows that  $p$  is constant in the two phase regime. The shear modulus is zero due to the fact that a finite shearing can be performed by a redistribution of the orientation of the collapsed meshes without a change of the elastic energy.

2.5. MEAN FIELD ESTIMATE AT FINITE TEMPERATURE. — In a first attempt to explore the effect of finite temperature  $\Theta$  (measured in units of  $kl_0^2/k_B$ ) we calculate the partition function of a network vertex. With the bond potential (3) the elastic energy (4) is *not* a harmonic function of the vertex positions. Calculating the partition function in the harmonic approximation, which becomes exact in the limit  $l_0 \rightarrow 0$ , is equivalent to the zero temperature analysis of static deformations [4]. For an alternative approximation, we neglect all correlations between the meshes. The single vertex partition function becomes

$$Z = \int dl_1 \int dl_2 \int dl_3 \frac{l_1 l_2 l_3}{2 A(l_1, l_2, l_3)} e^{-(f(l_1, l_2, l_3))/\Theta}. \quad (11)$$

The factor in front of the exponential gives the *a priori* statistical weight of a specific triangular conformation expressed in the bond length coordinates  $l_i$  (<sup>1</sup>). The three integrals can be performed numerically.

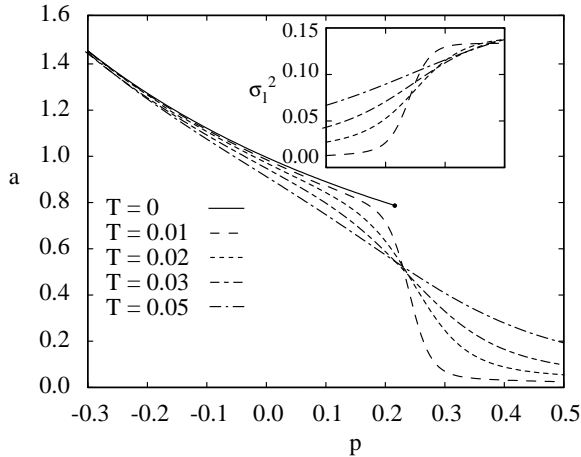


Fig. 2. — Area per vertex  $a$  as a function of pressure  $p$  resulting from mean-field calculation. The solid line corresponds to zero temperature (Eq. (5)). The inset shows the bond length fluctuations as given by equation (12) in the vicinity of the phase transition as a function of  $p$  (same units as in the main diagram).

Figure 2 shows the area *versus* pressure diagram resulting from this calculation together with the results from the zero temperature considerations given above. In this single mesh model, a strong decrease of the area per mesh indicates the presence of the phase transition even before the shear modulus vanishes in the harmonic approximation. Nevertheless, this decrease is smeared out even for low temperatures, as it should be expected in a one vertex model. The inset gives the square of the relative bond length fluctuations

$$\sigma_l^2 = \frac{\langle l^2 \rangle}{\langle l \rangle^2} - 1 \quad (12)$$

in the vicinity of the phase transition. When the pressure approaches the transition pressure, the bond length fluctuations increase rapidly. This one vertex model shows a reflection of the phase transition, but is definitely not capable of predicting reliable values of the elastic constants in the two-phase regime.

### 3. Monte Carlo Simulation

3.1. COLLAPSE TRANSITION. — The full coupling of the meshes can only be considered in a computer simulation. Therefore, we performed a Monte Carlo simulation with Boltzmann sampling for the Hooke's-law spring network in a constant area ensemble. The bounding box is periodic in  $x$ - and  $y$ -direction of a non-rectangular coordinate system. The periodicity of the box preserves the total area. Fixing the geometry of the boundary box imposes a deformation on the network. Bond crossing moves are rejected. The system of  $N = 20 \times 20$  vertices is prepared in equilateral conformation at the fixed area  $A$ . Then the system is allowed to evolve freely at constant temperature. In contrast to the simulation of Boal *et al.* [4], who have implemented a similar scheme for the pressure ensemble, the two phase regime is accessible to our simulation.

<sup>(1)</sup> This measure factor differs from an incorrect one used in reference [4].

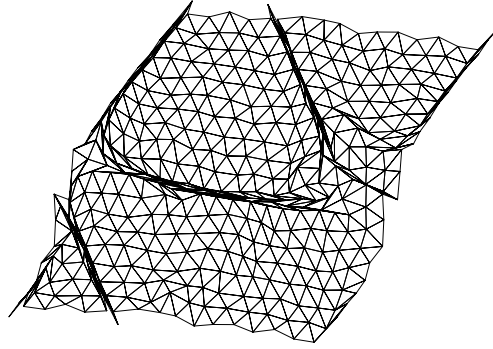


Fig. 3. — Typical configuration of the network at low temperature ( $\Theta = 0.01$ ) and compression to about half of the stress free area ( $a = 0.48$ ). The system is periodic at the upper and lower as well as at the left and right boundary.

Figure 3 shows a typical conformation in the low temperature two phase region. The collapsed domains form lines oriented along the preferred directions of the hexagonal net. Far away from these strings, the shapes of the triangles within the equilateral domains are affected only weakly by the presence of the collapsed meshes. However, the non collapsed triangles adjacent to the collapsed strings are distinctly non-equilateral.

This observation suggests that a domain boundary costs energy. In the lever rule calculation discussed in Section 2.4, the bond length in the equilateral phase fits neither the length of the short sides nor of the long side of the collapsed mesh. Figure 3 shows that the short sides are preferably in contact with the equilateral phase. The energy associated with this mismatch can be minimized by forming collapsed domains from several adjacent rows of meshes. Furthermore, the mismatch shears the triangles that are directly adjacent to the collapsed strings. This effect, which can be seen most clearly in Figure 3 above the horizontal string of collapsed meshes, limits the growth of the collapsed domains.

Due to these domain boundary effects, the collapse transition occurs by collective motions of chains of adjacent triangles. This fact explains the stability of the collapsed domains at low temperature observed in our simulations. Once a chain of meshes has collapsed, thermal fluctuations have to induce a collective motion in order to break up the string. The probability for this process is strongly reduced with increasing domain size.

3.2. ISOTROPIC COMPRESSION. — The elastic response of the network on deformations of the bounding box is evaluated by means of the pressure tensor defined by

$$P_{\alpha\beta} = \frac{\Theta}{a} \delta_{\alpha\beta} + \frac{1}{Na} \left\langle \sum_{ij} \frac{r_{ij\alpha} r_{ij\beta}}{|\mathbf{r}_{ij}|} f_{ij} \right\rangle \quad (13)$$

where  $ij$  counts the pairs of vertices connected by a spring,  $\mathbf{r}_{ij}$  denotes the bond vector between the connected pairs and  $f_{ij}$  the force exerted by the spring [13]. We performed two kinds of deformations: isotropic compression by a scaling of the boundary box and pure shearing. In the isotropic case,  $P_{11}$  and  $P_{22}$  are equal and give the lateral pressure  $p$ .

The average in (13) is performed by means of MC sampling. The sampling technique is somewhat different for the equilateral and the coexistence regime. In the equilateral regime configurations are picked from the sequence produced by a single MC run. At low temperature and high compression, for which a collapsed region exists, only one conformation of each

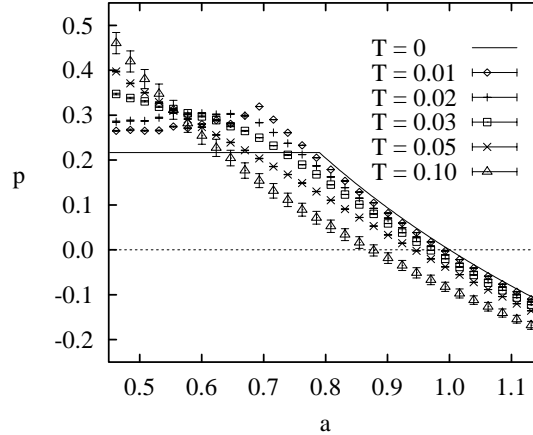


Fig. 4. — Pressure  $p$  as a function of the area per vertex  $a = A/N$  resulting from MC simulations. The solid line represents the  $\Theta = 0$  value from equation (5).

equilibrated system is collected. Using 500 such conformations, we average over different realizations of the collapsed domains. This procedure reflects the fact that at low temperatures the collapsed regions do not spontaneously break up once they have formed. The system shows enormous correlation times due to freezing of collapsed domains.

The  $p$ - $a$  diagram resulting from our simulations is shown in Figure 4. For low temperatures ( $\Theta = 0.01$  and  $\Theta = 0.02$ ) a pressure plateau indicates the collapse transition whereas for higher temperatures ( $\Theta \geq 0.03$ ) no indications of a phase transition are observed. Thus we find a critical temperature  $\Theta_c$  ( $0.02 < \Theta_c < 0.03$ ), above which the phase transition in our simulation disappears.

A closer inspection of Figure 4 shows that the pressure in the two phase regime is not exactly constant at small temperature. This small remaining area dependence of  $p$  may be due to domain boundary effects. A growing portion of non collapsed meshes becomes part of the phase boundary when  $a$  decreases. Figure 3 shows that these non collapsed triangles are not equilateral.

The lateral compression modulus can be extracted from the  $p$ - $a$  diagram by differentiation using equation (10). The result of a numerical differentiation of the data of Figure 4 using a four point neighborhood is given in Figure 5. For low temperature  $\Theta < \Theta_c$  the compression modulus drops to zero at  $a_c \simeq 0.79$  <sup>(2)</sup>. For temperatures larger than  $\Theta_c$ , the compression modulus stays non zero.

**3.3. SHEAR MODULUS.** — In order to extract the shear modulus from the simulations we shear the boundary box. Moving of the upper boundary of the simulation box, which has the length  $L$ , by  $\epsilon L$  to the right, we perform a shearing. The responding torque of the system is evaluated by means of the off diagonal elements of the pressure tensor. In this special geometry, the torque  $\tau$  generated by the network in response to the deformation is given by

$$\tau = NaP_{12}. \quad (14)$$

<sup>(2)</sup> The shoulder is artificially rounded by the smoothing method of numerical differentiation. As we have checked for selected points, the data is, apart from the shoulder, consistent with a computation of the compression modulus from the MC expectation value of the second derivative of the free energy with respect to the elements of the strain tensor.

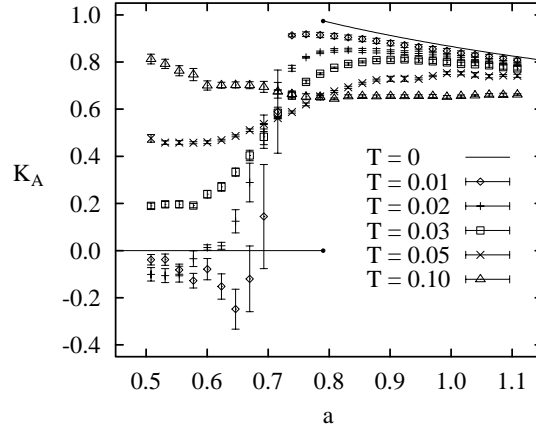


Fig. 5. — Compression modulus  $K_A$  resulting from numerical differentiation of the data in Figure 4 together with the  $\Theta = 0$  values (solid lines).

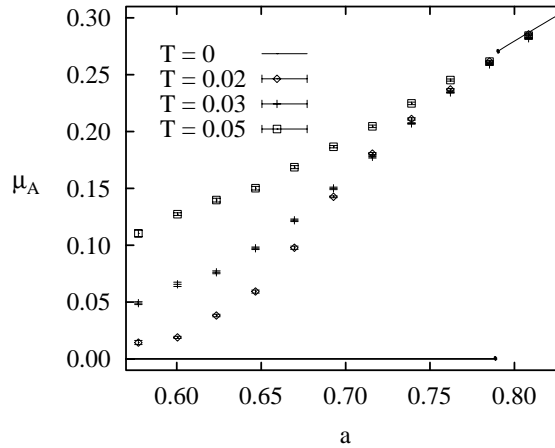


Fig. 6. — Shear modulus  $\mu_A$  as a function of the area per vertex  $a = A/N$  resulting from MC simulations for three different temperatures together with the  $\Theta = 0$  value.

For small shear deformations, the responding torque is proportional to the magnitude of the deformation. Besides a geometrical factor, the constant of proportionality is the shear modulus

$$\mu = \frac{\sqrt{3}}{2} \frac{\partial P_{12}}{\partial \epsilon}. \quad (15)$$

Figure 6 presents the results of our simulations. The solid line gives the  $\Theta = 0$  values from equation (9). It is a good approximation for  $a \gtrsim 0.8$ . In this regime, the shear modulus shows almost no temperature dependence.

For  $a < 0.8$  significant deviations from the behavior expected for  $\Theta = 0$  are found. Simulations for  $\Theta < \Theta_c$  are very time consuming due to the long correlation time induced by the stability of the collapsed domains. Therefore, we determined  $\mu_A$  for only one temperature below  $\Theta_c$  ( $\Theta = 0.02$ ). For this temperature, which is already close to the critical, we find no indications of a sharp drop of  $\mu_A$ . It decreases smoothly with decreasing  $a$  and seems to reach

zero asymptotically for small  $a$ . The signature of the collapse transition is a sudden increase of the temperature dependence of  $\mu_A$ .

In contrast to the compression modulus, which behaves, at least for small temperature, as it is expected in this kind of a phase transition, the shear modulus is not as strongly affected by the collapse transition. It does not show a sharp drop to zero at the entrance to the coexistence regime. The collapse of a mesh introduces a strong anisotropy to the remaining equilateral meshes. In the course of compression, more and more meshes collapse. The anisotropy induced by the already collapsed meshes imposes preferred directions for the following collapses. Meshes at the end zones of a collapsed string will tend to align with the string, meshes at some distance perpendicular to the string will collapse to one of the other two preferred directions of the hexagonal network. Therefore, in our simulation, the spatial distribution of collapsed domains shows strong correlations. Under certain conditions, these correlations produce regular pattern of collapsed meshes (see Figure 3). An odd distribution of collapsed meshes on the three preferred directions of the net, which is to some extent preferable to a shearing of the equilateral domains and indeed the reason for the slight decrease of the shear modulus at the entrance to the two phase regime, will partially destroy these pattern. This would again impose an anisotropic deformation of the remaining equilateral triangles and thereby cause a non zero shear modulus. The occurrence of such correlations may be an effect of our finite simulation box. If, however, the deformation of the equilateral phase induced by collapsed meshes decays slowly enough with the distance from the collapsed domain, which is not unusual for elastic interactions, it may also be an inherent feature of the system.

3.4. HIGH TEMPERATURE. — So far, we have discussed the system in a compressed state at low temperature. At temperatures  $\Theta > 0.03$ , we find no indications of a first order phase transition. In contrast to this observation Discher *et al.* [14] report on a first order phase transition between an equilateral phase and a completely collapsed phase for arbitrary finite temperatures. They perform a simulation of the equivalent system in the pressure ensemble. When the isotropic pressure exceeds a certain value, in their simulation the system collapses completely to one of the three preferred directions of the hexagonal network. In this transition, the symmetry of the system changes discontinuously from  $C_6$  to  $C_2$ . This first order transition can not end in a critical point due to the different symmetry of both phases.

The transition we study is the transition from the hexagonal phase to the coexistence phase of hexagonal domains and collapsed domains, which are regularly distributed to the three preferred directions of the hexagonal net. Assuming the equivalence of both ensembles, the existence of the transition from hexagonal to completely collapsed in the pressure ensemble for arbitrary finite temperature would imply an equivalent transition from the completely non collapsed to the coexistence phase in the area ensemble. However, we see a behavior of the system, which is akin to a critical point as the endpoint of a line of first order phase transition.

At present, we see two possible explanations for this difference with the results of Discher *et al.* [14]:

(i) Finite-size effects could mean that the simulations are still far from the thermodynamic limit of infinite system size. In this case, the position of the phase boundary and especially of the critical point should depend on the system size <sup>(3)</sup>.

(ii) Long-ranged elastic interactions are known to spoil the equivalence of the thermodynamic ensembles which holds only for sufficiently short-ranged interactions. In this case, a finite size effect is immanent to the system and vanishes never regardless of its actual size. If our network

---

<sup>(3)</sup> Even if the phase behavior turns out to depend only weakly on the system size, this finite size effect may still be relevant for the topologically closed skeleton of a red blood cell which is also a finite system.

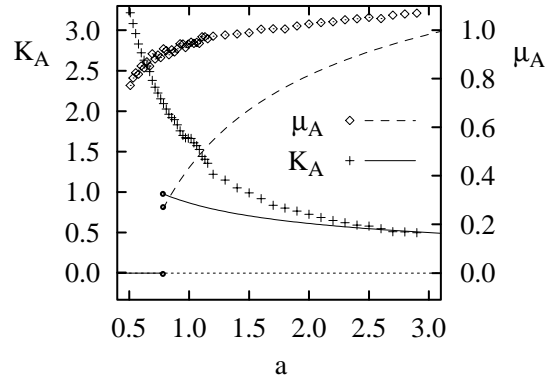


Fig. 7. — Compression modulus  $K_A$  and shear modulus  $\mu_A$  as a function of the area per vertex  $a = A/N$  resulting from MC simulations for  $\Theta = 1$ . The solid and the dashed line give the results for  $\Theta = 0$ .

system belongs to this class, a complete separation of the collapsed domains and the hexagonal domains, as it is usually expected in the thermodynamic limit due to the decreasing importance of the domain boundaries, is not possible. The two ensembles could then show different phase behavior even for very large systems <sup>(4)</sup>.

The precise character of the phase transition in the area ensemble should be resolved in the future by simulations of far larger systems.

The elastic properties of the network deviate significantly from the values of the harmonic theory discussed in Section 2.4 even when the network is slightly stretched. As a representative example, we show in Figure 7 the compression and the shear modulus at  $\Theta = 1$  in a wide range of  $a$ . Both,  $K_A$  and  $\mu_A$  are smooth and non vanishing functions of  $a$ . Only for  $a \gtrsim 3$ , equations (8, 9), which hold exactly in the limit  $a \gg 1$ , become good approximations of the simulation results.

#### 4. Application to Red Blood Cell Skeletons Models

We now discuss how our model relates to previous models of the red blood cell skeleton. Isolated spectrin molecules are flexible, water-soluble macromolecules with a large number of charged side groups [15]. In modeling the spectrin network, one has to account for the effective inter- and intra-molecular interactions as well as for the presence of the bilayer and of counter-ions.

The basic model of the spectrin network uses expressions from classical rubber elasticity [16]. Implicitly, the cytoplasm is treated as a  $\Theta$ -solvent in which the network strands behave as ideal Gaussian chains. The shear elastic properties of a network of ideal entropic springs can be calculated analytically [17]. Later refinements took quite opposite views on the importance of the polyelectrolyte character of spectrin. Stokke *et al.* [18] treated the network as an ionic gel. In *bad* solvents the counter-ion osmotic pressure leads to phase separation and a vanishing compression modulus of the network. Other groups have completely ignored electrostatic interactions and modeled spectrin as a flexible polymer in a *good* solvent [19–21]. This is motivated by the strong screening under physiological conditions and the observation that the isolated cytoskeleton is stable, shows no signs of (local) collapse [6], and adopts conformations similar to those found in simulations of closed two-dimensional triangular networks of self-avoiding bead-spring chains [22]. The elastic properties of such a network in contact with

<sup>(4)</sup>In a note added to [14], the possibility that the two ensembles are not equivalent has also been suggested.

an impenetrable surface and under zero external pressure were measured in extensive computer simulations [20] and can be understood on the basis of the  $c^*$ -theorem [1,21].

Conceptually, one should distinguish between microscopic and mesoscopic (or effective) models. The first approach relies on simulations of molecular models of the spectrin network. In the comprehensive study by Boal [20], the spectrin molecules are modeled as bead-spring-chains, explicitly including volume interactions between beads and the presence of the surface. In principle, the extraction of the elastic properties of the model network and the inclusion of molecular detail into the model are limited only by the available computing resources which, in practice, can be a severe limitation.

Mesoscopic or effective models, like the classical theories of rubber elasticity, start with a networks of entropic springs. The difficulty lies in mapping the microscopic interactions on appropriate spring equations and (possibly) interactions between neighboring springs. Simulations of microscopic models therefore provide valuable test cases to check the predictions and the interpretation of parameters for a mesoscopic model. Once the mapping is understood, the accessible time and length scales are orders of magnitude larger than for microscopic models, even if a mesoscopic model cannot be solved analytically. Such models can be treated either by methods of computer simulations [4], affine theory [23] or the analysis of static deformations [24]. While computer simulations are capable of including mesh fluctuations and topological constraints, these effects are left out by affine theory and the static analysis.

We will now relate our simulation to the simulation of Boal [20]. The macroscopic state of the network, characterized by the vertex area density  $\rho = N/A$  and the temperature  $T$ , is known. For our model, we have to specify appropriate values of the parameters  $\Theta = k_B T / k l_0^2$  and  $a = 2/\sqrt{3} \rho l_0^2$ , from a comparison to the (approximately) known single chain characteristic of the network strands used in the model of Boal. Then we can use our results for the isotropic shear and compression modulus and their dependence on isotropic compression for a comparison with the microscopic model.

In the case of self-avoiding chains, values for  $\Theta$  and  $a$  can be deduced by comparison to the Redner-des Cloizeaux (RdC) expression for the end-to-end distance distribution of SAW in a halfspace with both endpoints on the limiting surface (in the following denoted as  $3d/2$ ) [23,25]. The RdC force-elongation relation is given by

$$f(x) = -\frac{k_B T}{\langle r^2 \rangle_{3d/2}} (\theta x^{-1} - t K^t x^{t-1}), \quad (16)$$

where the end-to-end distance  $x$  is measure in units of the root-mean-square end-to-end distance  $\sqrt{\langle r^2 \rangle_{3d/2}}$ ,  $t \simeq 2.5$  and  $\theta \simeq 0.35$  are (effective) exponents related to the SAW critical exponents, and  $K \simeq 1$  a numerical normalization constant. In harmonic approximation, equation (16) corresponds to Hooke's law springs with  $l_0 \simeq 0.5 \sqrt{\langle r^2 \rangle_{3d/2}}$  and  $k \simeq 3.8 k_B T / \langle r^2 \rangle_{3d/2}$ . This leads to a reduced temperature  $\Theta \simeq 1.1$ .

In the absence of external forces, the size of the network in the simulation of Boal measured in our units is  $a \simeq 3.2 \langle r^2 \rangle_{3d/2} / l_0^2 \simeq 13$  [20]. This finding is used to determine the second of our parameters. As Figure 7 shows, this value for  $a$  is large enough to neglect the effect of topological constraints and mesh fluctuations. Thus equation (9) gives a good approximation for the shear modulus. Inserting the natural units, it predicts  $\mu = 5.2 k_B T / \langle r^2 \rangle_{3d/2}$ . This is in excellent agreement with  $\mu = 5.1 k_B T / \langle r^2 \rangle_{3d/2}$  from the junction affine model used in reference [21], which inherently makes the assumption of negligible mesh fluctuations, and in good agreement with  $\mu = 4.2 k_B T / \langle r^2 \rangle_{3d/2}$  from the extrapolation of simulation data by Boal [20] <sup>(5)</sup>.

---

<sup>(5)</sup> see reference [21] for a discussion of possible finite strand length effects in [20].

Our model can account only for the shear elastic properties of the network and not for the compression modulus.  $K_A/\mu_A$  predicted by our model is approximately 0.2 while in the simulation  $K/\mu \simeq 1.7$ . In order to adjust the lateral extension of our network to the situation found in the microscopical simulation, an internal pressure  $p_{in} \simeq -1.2$  is necessary. The present example illustrates that choosing a non-zero internal pressure in order to adjust a given value of network stretching is sufficient to extract the shear modulus but may lead to erroneous results for the compression modulus.

Finally, we assess the consistency of the recent effective model by Hansen *et al.* [24]. This finite element description of the network emphasizes the single chain elasticity and the influence of a random network topology. Thermal fluctuations of the meshes, however, are neglected. The network is assumed to be in a *relaxed* initial state, which means  $p = 0$  and  $a = 1$ , if we neglect the influence of randomness. This assumption is obviously in contrast to the outcome of the simulation of Boal. Due to this assumptions, the equilibrium length of the spectrin molecules in the RBC network of about 70nm is identified with  $l_0$ . For  $\Theta = 0$  and  $a = 1$ , equation (9) gives  $\mu_A = \sqrt{3}/4 \simeq 0.43$  in units of  $k$ . In this model, the spring constant  $k$  has to be extracted from an external source, which is the measured value of  $\mu$ . After assigning values to  $k$  and  $l_0$ , the value for  $\Theta$  can be calculated. The crucial question is, whether this value is consistent with the initial assumption of negligible thermal fluctuations. Using the value for the shear modulus  $\mu \simeq 6.6 \times 10^{-3}$  dyn/cm published by Waugh *et al.* [26] leads to  $k \simeq 1.5 \times 10^{-2}$  dyn/cm, which means  $\Theta \simeq 0.05$ . Figure 6 shows that for such low value of  $\Theta$  and  $a \gtrsim 0.8$  the influence of  $\Theta$  on the shear modulus is indeed negligible. However, for  $a < 0.8$  it is not. If we take a value for  $\mu$  from the flicker analysis by Strey *et al.* [11], which is typically two orders of magnitude smaller than the results from micropipette experiments, the assumption of negligible fluctuations is inconsistent even at  $a = 1$ . Thus, in contrast to the affine model, where the negligible effect of thermal fluctuations can be justified *a posteriori* by the harmonic character of the network at sufficiently high values of  $a$ , this assumption is questionable in the Hansen model.

In conclusion, our simple model with its two parameters  $\Theta$  and  $a$  allows a classification of the different effective models for the RBC membrane skeleton. Typical for all those models, which deduce the elastic properties of the network from single chain properties alone, is the fact that they give unreasonable results for the local compressibility. Even though this network compressibility is in any case small compared to the compressibility of the bilayer and can therefore be neglected for the question how the membrane area changes when a certain pressure is applied to the membrane as a whole, it is crucial for the problem how the network reacts on cell deformations. Modeling the membrane network by a system of connected springs, which is an obvious idea especially for an investigation of the effects of *strong* and *anisotropic* deformations, has to include some feature of the chain-chain interactions, which mainly contribute to the network compressibility. This could be done by replacing the internal pressure in the second term on the right hand side of equation (1) by a more realistic expression, which considers the dependence of the chain-chain interactions on the local chain density.

## 5. Conclusions

The mechanical properties of a hexagonal network of springs are in a certain range of temperature and compression strongly influenced by the presence of a configurational phase transition. Lateral compression of the network induces a sharp collapse of chains of net meshes. With increasing temperature we find a critical point, above which the phenomenon disappears.

Below this critical temperature and beyond a threshold value of compression, the area of the net can be decreased without a change in internal pressure due to a growing fraction

of collapsing meshes. In this state, the network can easily be sheared by a redistribution of energetically equivalent but geometrically distinct collapsed conformations. Above the critical temperature the network shows elastic response to area expansion as well as to shear. This elasticity of the hexagonal network of Hooke's-law springs with non-zero equilibrium length under compression is of entropic origin.

The difference in the elastic behavior between the stretched and the compressed network is a consequence of the difference in the fluctuations of mesh shapes. In the strongly stretched case, the position of an individual fluctuating vertex remains in the vicinity of its equilibrium position. The system behaves like a harmonic solid, showing no influence of temperature on the elastic properties. Therefore the zero temperature estimates are in good agreement with the Monte Carlo simulations for finite temperature [4]. With decreasing tension, shear fluctuations become more important. For non-zero equilibrium length, these fluctuations are anharmonic which implies a temperature dependence of the elastic constants.

One application of our network model is to the skeleton of red blood cell membranes. The advantage of such a network model is that it includes fluctuations of the mesh points while it is not as time consuming as the simulation of more microscopic models. Identifying the model parameters with one particular microscopic model, we find good agreement for the shear modulus. For a full description of the elastic behavior including the compression modulus, especially under the condition of *anisotropic* deformation, a physically motivated concept has to be developed how to include chain-chain interactions beyond an isotropic tension into such an effective model. Only then will it be possible to specify the conditions under which the collapse transition discussed here may become relevant for strongly deformed red blood cell membranes.

### Acknowledgments

We thank E. Sackmann and T.M. Fischer for helpful discussions. W.W. and R.E. thank K. Kehr from IFF, Forschungszentrum Jülich for hospitality.

*Note added:* After the submission of this work, we received a preprint by Discher *et al.* [14], who investigate the collapse transition in the pressure ensemble. They find that a first-order transition persists at temperatures far above our critical point. Possible reasons for this difference with our results are discussed in the current Section 3.4.

### References

- [1] de Gennes P.G., *Scaling Concepts in Polymer Physics* (Cornell University Press, Ithaca and London, 1979).
- [2] *Statistical Mechanics of Membranes and Surfaces*, D. Nelson, T. Piran and S. Weinberg, Eds. (World Scientific, Singapore, 1989).
- [3] Boal D.H., Seifert U. and Zilker A., *Phys. Rev. Lett.* **69** (1992) 3405.
- [4] Boal D.H., Seifert U. and Shillcock J.C., *Phys. Rev. E* **48** (1993) 4274.
- [5] Steck T.L., *Cell Shape: Determinants, Regulation and Regulatory Role* (Academic Press, New York, 1989).
- [6] Svoboda K., Schmidt C.F., Branton D. and Block S.M., *Biophys. J.* **63** (1992) 784.
- [7] Chabanel A. *et al.*, *Biophys. J.* **44** (1983) 171.

- [8] Evans E., *Biophys. J.* **30** (1980) 265.
- [9] Discher D.E., Mohandas N. and Evans E.A., *Science* **266** (1994) 1032.
- [10] Zilker A., Ziegler M. and Sackmann E., *Phys. Rev. A* **46** (1992) 7998.
- [11] Strey H., Peterson M. and Sackmann E., *Biophys. J.* **69** (1995) 478.
- [12] Cates M.E. and Deutsch J.M., *J. Phys. France* **47** (1986) 2121.
- [13] Allen M.P. and Tildesley D.J., *Computer Simulation of Liquids* (Oxford University Press, Oxford, 1987).
- [14] Discher D.E., Boal D.H. and Boey S.K., *Phys. Rev. E* **55** (1997) 4762.
- [15] Speicher D.W. and Marchesi V.T., *Nature* **311** (1984) 177.
- [16] Evans E.A., *Biophys. J.* **13** (1973) 926.
- [17] Treloar L.R.G., *The Physics of Rubber Elasticity* (Clarendon Press, Oxford, 1975).
- [18] Stokke B.T., Mikkelsen A. and Elgsaeter A., *Eur. Biophys. J.* **13** (1986) 203.
- [19] Petsche I.B. and Grest G.S., *J. Phys. I France* **3** (1993) 1741.
- [20] Boal D.H., *Biophys. J.* **67** (1994) 521.
- [21] Everaers R., Graham I.S., Zuckermann M.J. and Sackmann E., *J. Chem. Phys.* **104** (1996) 3774.
- [22] Schmidt C.F. *et al.*, *Science* **259** (1993) 952.
- [23] Everaers R., *J. Phys. II France* **5** (1995) 1491.
- [24] Hansen J.C., Skalak R., Chien S. and Hoger A., *Biophys. J.* **70** (1996) 146.
- [25] de Cloizeaux J., *Les Polymères en Solution* (Les Éditions de Physique, Les Ulis, 1987).
- [26] Waugh R. and Evans E.A., *Biophys. J.* **26** (1979) 115.